VI. ELECTRODYNAMICS OF MEDIA[*]

Academic and Research Staff

Prof. L. J. Chu	Prof. J. I. Glaser	L. Frenkel
Prof. H. A. Haus	Prof. J. A. Kong	R. H. Rines
	Prof. P. Penfield, Jr.	

Graduate Students

B. L. Diamond	M. A. Guerra	E. E. Stark, Jr.
H. Granek	P. W. Hoff	C. M. Watson
	E. R. Kellet, Jr.	

A. PARAMETRIC CROSS-MODULATION EFFECTS IN GAS LASERS

Many phenomena in gas lasers have been explained by rate equations, which show "hole burning" in the population inversion, but do not consider time variation of the population inversion when two, or more, oscillations coexist simultaneously within the medium.

In recent experiments by M. Guerra,[1] an external signal from a single-frequency, tunable, Spectra Physics laser was injected into a long He-Ne laser oscillating in 7 or 8 modes at 6328 Å. When this signal fell near one of the oscillating modes the output showed, in addition to the amplified input signal, a signal with a frequency located symmetrically with respect to the signal frequency on the opposite side of the gain curve of the laser medium. This cross-modulation "signal" cannot be explained if it is assumed that the negative conductivity of the laser medium is time-independent. A density matrix analysis of a Doppler-broadened two-level system in the presence of two simultaneous oscillations showed that the time dependence of the negative conductivity can be surprisingly large because of a synchronism effect.

In this report we shall analyze the density matrix equations in the presence of two traveling waves of different frequencies. A perturbation signal is injected, and the self-term (at the frequency of the injected signal) of the polarization density, as well as the cross term of the polarization density, resulting from intermodulation products, is evaluated. The signal-dependent parts of the self-term and cross term are found to be comparable in amplitude. Integration of these terms over the velocity distribution reduces the magnitude of the latter term compared with the magnitude of the former in the ratio of the homogeneous linewidth to the Doppler linewidth. It is surmised that the coupling of the modes in a laser cavity by the intermodulation products is responsible for the self-pulsing observed by P. W. Smith.[2]

We start with the density matrix of a system with a very fast relaxation out of its lower level so that this level may be considered essentially empty. Denoting the upper level by the subscript 2, the lower level by the subscript 1, we have (note $\rho_{11} \cong 0$)

$$\left(\frac{\partial}{\partial t} + v \frac{\partial}{\partial z}\right)\rho_{22} = -\{jV_{12}\rho_{21} + \text{c. c.}\} - \left(\rho_{22} - \rho_{22}^o\right)/T_1 \tag{1}$$

$$\left(\frac{\partial}{\partial t} + v \frac{\partial}{\partial z}\right)\rho_{12} = -\frac{\rho_{12}}{T_2} + j\omega_{12}^o\rho_{12} + jV_{12}\rho_{22}. \tag{2}$$

The matrix elements ρ_{ij} are functions of time, space, and velocity v. The center frequency of the Doppler-broadened profile is ω_{12}^o.

We introduce two fields, at frequencies ω_a and ω_b, so that the matrix element V_{12} becomes

$$V_{12} = V_a e^{j(\omega_a t - k_a z)} + V_b e^{j(\omega_b t + k_b z)}. \tag{3}$$

Wave b runs in the negative z-direction, wave a in the positive z-direction, since we take k_a and k_b to be positive.

We shall solve (1) and (2) by a process of successive approximations. Since V_{12} has two space and time dependences, we conclude that ρ_{12} will have also two such dependences in the steady state:

$$\rho_{12} = \rho_{12}^a \exp j(\omega_a t - k_a z) + \rho_{12}^b \exp j(\omega_b t + k_b z). \tag{4}$$

Introducing this Ansatz into (2), we have

$$\rho_{12}^a = \frac{j\rho_{22}^o V_a}{j(\Delta\omega_a) + \frac{1}{T_2} - jvk_a} \tag{5}$$

$$\rho_{12}^b = \frac{j\rho_{22}^o V_b}{-j(\Delta\omega_b) + \frac{1}{T_2} + jvk_b}, \tag{6}$$

where

$$\Delta\omega_a = \omega_a - \omega_{12}^o > 0 \tag{7}$$

$$\Delta\omega_b = -\left(\omega_b - \omega_{12}^o\right) > 0, \tag{8}$$

in anticipation of the fact that ω_a and ω_b will lie on opposite sides of the Doppler profile. When (5) and (6) are introduced into (1), the product $\rho_{12}V_{21}$ and its complex conjugate each produce two time- and space-independent terms $\rho_{12}^a V_a^*$, $\rho_{12}^b V_b^*$ and their complex conjugates, as well as two terms with space-time dependence. Hence we find

$$\Delta\rho_{22} = \rho_{22} - \rho_{22}^o$$

$$= \Delta\rho_{22}^{oo} + \Delta\rho_{22}^{ab} \exp j[(\omega_a-\omega_b)t-(k_a+k_b)z] + c.c., \tag{9}$$

where

$$\Delta\rho_{22}^{oo} = T_1\left[j\rho_{12}^a V_a^* + j\rho_{12}^b V_b^* - j\rho_{12}^{a*}V_a - j\rho_{12}^{b*}V_b\right]$$

$$= -2\frac{T_1}{T_2}\left\{\frac{\rho_{22}^o|V_a|^2}{(\Delta\omega_a-vk_a)^2 + \frac{1}{T_2^2}} + \frac{\rho_{22}^o|V_b|^2}{(\Delta\omega_b-vk_b)^2 + \frac{1}{T_2^2}}\right\} \tag{10}$$

This is the familiar lowering of the population inversion because of depletion by the laser field. The term with the space-time dependence $\exp j[(\omega_a-\omega_b)t-(k_a+k_b)z]$ is

$$\Delta\rho_{22}^{ab} = \frac{j\rho_{12}^a V_b^* - j\rho_{12}^{b*}V_a}{j[(\omega_a-\omega_b)-v(k_a+k_b)] + \frac{1}{T_1}}$$

$$= -\frac{V_a V_b^* \rho_{22}^o}{j[(\omega_a-\omega_b)-v(k_a+k_b)] + \frac{1}{T_1}}\left\{\frac{1}{j(\Delta\omega_a-vk_a) + \frac{1}{T_2}} + \frac{1}{j(\Delta\omega_b-vk_b) + \frac{1}{T_2}}\right\}. \tag{11}$$

Note that this term need not be smaller than the term $\Delta\rho_{22}^{oo}$. Indeed, consider the velocity groups v for which the hole-burning is most pronounced, $v_a = \Delta\omega_a/k_a$, $v_b = \Delta\omega_b/k_b$. If $\Delta\omega_a = \Delta\omega_b$ (that is, when the two frequencies are located symmetrically with respect to the Doppler profile) these two groups involve the same particles. For these particles, assuming that $\Delta\omega_a = \Delta\omega_b$, $\omega_a - \omega_b = 2\Delta\omega_a = 2vk_a = v(k_a+k_b)$, we have

$$\Delta\rho_{22}^{oo} = -2T_1T_2\rho_{22}^o\left\{|V_a|^2 + |V_b|^2\right\} \tag{12}$$

$$\Delta\rho_{22}^{ab} = -2T_1T_2V_a V_b^* \rho_{22}^o. \tag{13}$$

Thus, if $V_a = V_b$, then $\left|\Delta\rho_{22}^{ab}\right| = \frac{1}{2}\Delta\rho_{22}^{oo}$. Hence, these very same particles experience

a strong fluctuation in their inversion. This fluctuation is the result of a synchronism effect: Note that for these particles, the total time derivative $\frac{\partial}{\partial t} + v \frac{\partial}{\partial z}$ in (1) vanishes. This means that the time variation of the driving term in Eq. 1, as viewed by the traveling particle in its own frame of reference, is zero, the driving term is independent of time and hence affects the ρ_{12} of this particle maximally. This is true even though the source, as viewed in the laboratory frame, is time- and space-dependent.

We shall now investigate the space-time dependence of the polarization density when a small signal field is injected with the space-time dependence $V \exp j(\omega t + kz)$. Starting with the perturbed value of ρ_{22}, (9), we have for ρ'_{12}, the component of ρ_{12} with the space-time dependence $\exp j(\omega t + kz)$:

$$\rho'_{12}(\omega, v) = \frac{jV\left[\rho_{22}^{o} + \Delta\rho_{22}^{oo}\right]}{j\left[\left(\omega - \omega_{12}^{o}\right) + vk\right] + \frac{1}{T_2}} .$$ (14)

In addition to this component, there are cross-modulation components attributable to the product of the probe-signal term in V_{12}, and the space-time dependent terms in $\Delta\rho_{22}$. The term of ρ_{12} with the space-time dependence $\exp j[(\omega+\omega_a-\omega_b)t-(k_a+k_b-k)z]$, which we denote by ρ''_{12}, has the amplitude

$$\rho''_{12} = \frac{jV\Delta\rho_{22}^{ab}}{j\left[\left(\omega+\omega_a-\omega_b-\omega_{12}^{o}\right) - v(k_a+k_b-k)\right] + \frac{1}{T_2}} .$$ (15)

In order to find the net polarization, we must integrate ρ'_{12} and ρ''_{12} over all velocities. $\Delta\rho_{22}^{ab}$ peaks at the velocity $v = \Delta\omega_a/k_a \cong \Delta\omega_b/k_b$, when $\omega_a = \omega_b$ ($k > 0$). Let us compare the magnitudes of the nonlinear contributions to the polarization, proportional to $\int \rho_{12}\, dv$, at frequencies ω and $\omega + \omega_a - \omega_b$, when $\omega = +\omega_b$. We have

$$\int \rho'_{12}\, dv = \int dv\ \frac{jV\Delta\rho_{22}^{oo}}{-j(\Delta\omega_b-vk) + \frac{1}{T_2}}$$

$$= -jV \int dv\ \frac{2\frac{T_1}{T_2}\rho_{22}^{o}\left\{|V_a|^2+|V_b|^2\right\}}{\left[-j(\Delta\omega_b-vk) + \frac{1}{T_2}\right]\left[(\Delta\omega_b-vk)^2 + \frac{1}{T_2^2}\right]} .$$ (16)

At frequency $\omega + \omega_a - \omega_b = \omega_a$, the polarization is proportional to

$$\int \rho''_{12} \, dv = \int dv \, \frac{jV\Delta\rho^{ab}_{22}}{j(\Delta\omega_a - vk) + \frac{1}{T_2}}$$

$$= -jVV_aV^*_b \int dv \, \frac{\rho^o_{22}}{\left[j(\Delta\omega_a - vk) + \frac{1}{T_2}\right]^2 \left[j(\Delta\omega_a - vk) + \frac{1}{2T_1}\right]} \, . \tag{17}$$

The simplest procedure, leading to an easy integration, is to assume a Lorentzian profile for the velocity distribution

$$\rho^o_{22}(v) = \frac{\rho^o_{22}(o) \, v_o}{2\pi\left[v^2 + \left(\frac{v_o}{2}\right)^2\right]} \, , \tag{18}$$

where v_o is the half-width of the velocity profile. We find for the nonlinear contribution to $\int \rho'_{12} \, dv$, using the residue theorem:

$$\int \rho'_{12} \, dv = -j2V \frac{T_1}{T_2} \rho^o_{22}(0) \left(|V_a|^2 + |V_b|^2\right) \left\{ \frac{v_o T_2^2}{4k\left[\left(\frac{v_o}{2}\right)^2 + \frac{1}{k^2}\left(\Delta\omega_b - \frac{j}{T_2}\right)^2\right]} \right.$$

$$\left. + \frac{1}{\left[\frac{1}{T_2} + \frac{v_o k}{2} - j\Delta\omega_b\right]\left[\left(\Delta\omega_b + j\frac{v_o k}{2}\right)^2 + \frac{1}{T_2^2}\right]} \right\} \, .$$

Similarly, for $\int \rho''_{12} \, dv$ we find

$$\int \rho''_{12} \, dv = \frac{-VV_aV^*_b \rho^o_{22}(0)}{2\left[\left(\frac{1}{T_2} + \frac{v_o k}{2}\right) + j\Delta\omega_a\right]^2 \left[\left(\frac{1}{2T_1} + \frac{v_o k}{2}\right) + j\Delta\omega_a\right]} \, .$$

Assuming $|V_a| = |V_b|$, $T_1 = T_2$, $\Delta\omega \gg 1/T_2$, and $v_o k \approx \frac{n}{T_2}$ [$n \approx 10$ in the He-Ne laser], we have

$$\left| \int \rho'_{12} \, dv \right| \approx \frac{4V|V_a|^2 kv_o T_2^2 \rho^o_{22}(0)}{\Delta\omega_a^2} \approx \frac{4V|V_a|^2 nT_2 \rho^o_{22}(0)}{(\Delta\omega_a)^2}$$

$$\left| \int \rho''_{12} \, dv \right| \approx \frac{V |V_a|^2 \, \rho^o_{22}(0)}{2(\Delta \omega_a)^3} \, .$$

Thus

$$\frac{\left| \int \rho''_{12} \, dv \right|}{\left| \int \rho'_{12} \, dv \right|} \approx \frac{1}{8 n \Delta \omega_a T_2} \, .$$

The cross-modulated component of the polarization caused by the probe signal is less than the polarization at the probe signal frequency in the ratio of the homogeneous to the inhomogeneous linewidths.

Since $\omega = \omega_b$ and $k = k_b$, the space-time dependence of the ρ''_{12}-term is $\exp j(\omega_a t - k_a z)$. An injected probe signal at frequency ω_b produces a component of polarization at frequency ω_a. Thus, the gain at one frequency depends upon the magnitude of the signal at another frequency. This is the type of interaction required for mode locking, and self-pulsing in lasers.

H. A. Haus, E. E. Stark, Jr.

References

1. M. A. Guerra, "Parametric Effects in the Helium-Neon Gas Laser," S. M. Thesis, M. I. T., September 1969. [See also Sec. VI-B of this report.]

2. P. W. Smith, "The Self-Pulsing Laser Oscillator," IEEE J. Quantum Electronics, Vol. QE-3, p. 627, November 1967.

B. PARAMETRIC EFFECTS IN THE HELIUM-NEON GAS LASER

This report deals with a parametric effect in the Helium-Neon gas laser. A signal of a certain frequency is injected into the cavity of a laser in multimode operation. The effect of this signal at a frequency symmetrically located with respect to the center of the Doppler line of the laser is then studied.

It can be shown using the density matrix equations that when a signal is injected into a multimode laser the output increases at the frequency of the injected signal and at the frequency symmetrically located with respect to the center of the Doppler line.[1] This is in contradiction to the steady-state rate equation approach which predicts that the output should be decreased at the symmetrically located frequency. A simplified analysis using the density matrix approach was presented in Section VI-A of this report, using only two countertraveling waves at two frequencies. A similar, but lengthier, analysis using standing waves is presented in the author's thesis.[1]

Experimentally a signal was injected from a single mode Helium-Neon laser into the cavity of another longer Helium-Neon laser. This second laser was oscillating in several different modes simultaneously. The frequency of operation of the first laser could be varied by manually changing an external control. This frequency variable laser was a Spectra-Physics Model 119. The other laser was built here at M.I.T. and had a cavity length of 1.1 meters while the mirror radii were 2 meters. A lens system was designed to mode match the two resonant cavities. A Faraday rotator was used to isolate the cavities from one another. The Spectra-Physics signal was injected into the cavity of the long Helium-Neon laser and the combined output was directed into a Spectra-Physics spectrum analyzer. The resultant was then displayed on an oscilloscope. The operating modes appear as spikes on the oscilloscope screen. The horizontal position on the scope display was a measure of the frequency of the modes. The experimental setup is shown in Fig. VI-1.
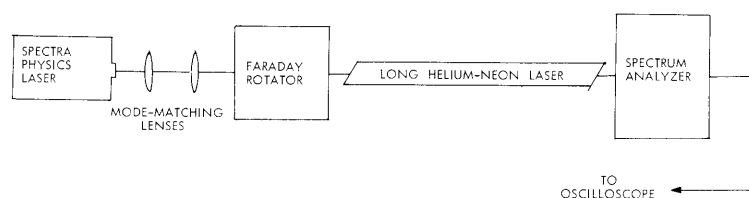

Fig. VI-1. Experimental layout.

The intention was to manually vary the frequency of the Spectra-Physics laser until it coincided with one of the modes of operation of the second laser. Then we could monitor the output at that frequency and at the symmetrically located frequency with respect to the center of the Doppler line of the second laser. This means of observation was complicated because the "comb" of frequencies of the long laser displayed on the oscilloscope jumped back and forth very rapidly. Consequently, it was virtually impossible to tell when the spike from the Spectra-Physics laser lined up with one of the spikes of the long He-Ne laser. To circumvent this difficulty, we used the memory storage capability on the oscilloscope. The frequency of the Spectra-Physics laser was adjusted to fall within the range swept out by the comb of the long He-Ne laser. Then the comb's sweeping back and forth across the face of the oscilloscope was equivalent to varying the frequency of the Spectra-Physics laser. When the spike of the Spectra-Physics laser coincided with one mode of the second laser a sharp increase in the output occurred. So, if there was such a coincidence it would show up on the oscilloscope memory as a large spike rising above the normal envelope swept out by the trace of the oscilloscope. Occasionally, not one but two spikes would appear which were
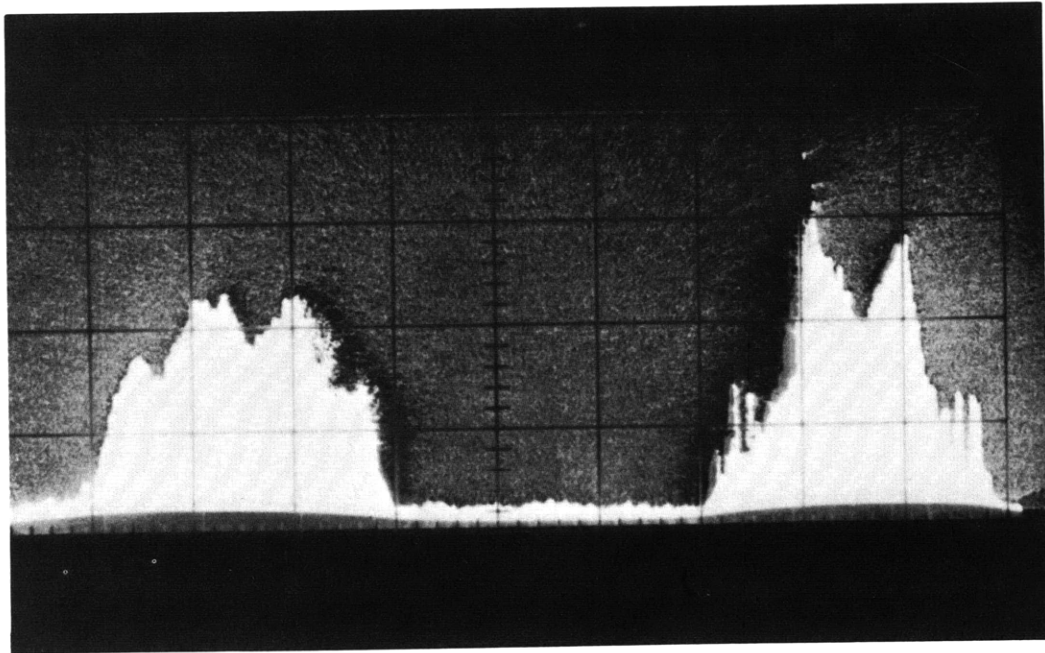
(a) (b)

Fig. VI-2. Oscilloscope traces with (b) and without (a)
Spectra-Physics laser on.
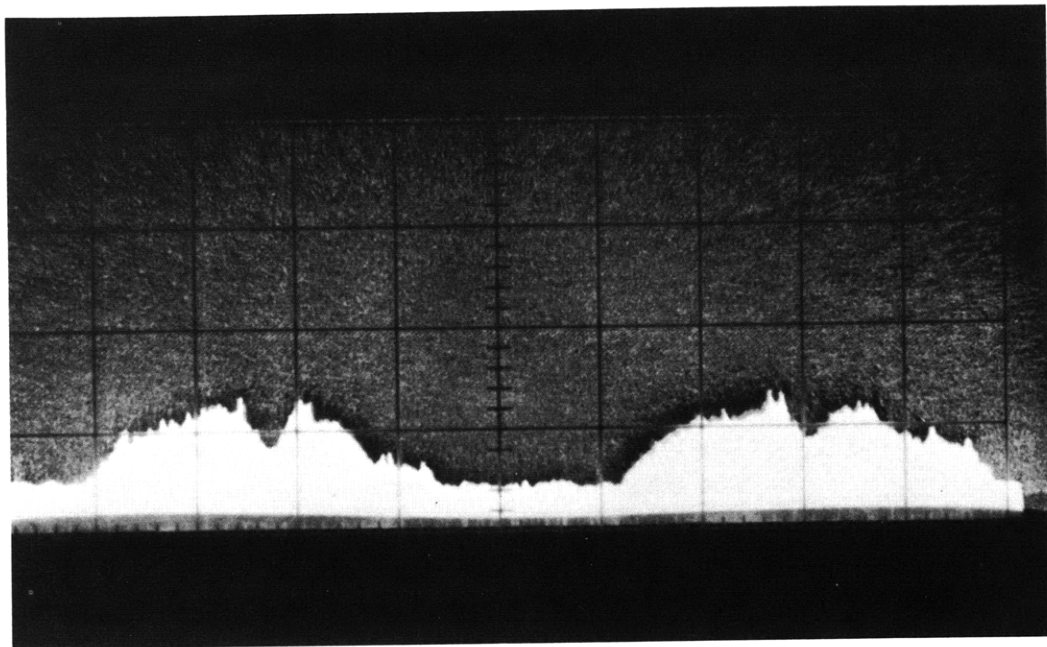
(a) (b)

Fig. VI-3. Reproducibility check.

symmetrically located on the Doppler-broadened line. This is evidence of the effect we are studying.

Just such an occurrence is shown in Fig. VI-2. The trace on the right is with the Spectra-Physics laser on and the one on the left is with it off. The large peak half a box to the left of the center in Fig. VI-2b is that due to the Spectra-Physics laser. The peak just to the right of center in Fig. VI-2b is considerably higher than the corresponding peak in Fig. VI-2a. This is an indication of the parametric effect and could only be due to the presence of the Spectra-Physics laser signal.

The reproducibility of the time-averaged envelope is indicated in Fig. VI-3. Both traces were done with the Spectra-Physics laser off.

For further experimental evidence of this effect and a more detailed theoretical analysis one should consult the thesis upon which this report is based.

M. A. Guerra

References

1. M. A. Guerra, "Parametric Effects in the Helium-Neon Gas Laser," S.M. Thesis, Department of Electrical Engineering, M.I.T., September 1969.

C. USE OF ADDITION THEOREMS FOR ELECTROMAGNETIC FIELD SYNTHESIS ON CIRCULAR CYLINDERS AND SPHERES

1. Introduction

This report is concerned with the use of addition theorems for the synthesis of time-harmonic electromagnetic field distributions on circular cylinders or spheres. By means of addition theorems a field distribution on a circular cylinder or sphere can be synthesized in terms of waves radiating from an eccentric center located inside. Solution of this synthesis problem is important for the design and evaluation of focal region feed antennas for circular-cylindrical or spherical metallic reflectors on a transmitting basis.[1] The design goal is a fan-beam or pencil-beam radiation pattern with a narrow beamwidth and low sidelobes which can be steered by rotating the feed on a circular arc. Use of the eccentric coordinate systems extends the transmitting synthesis approach of Ricardi who employed concentric spherical coordinates.[2]

The main result of this report is that the addition theorems provide exact synthesis and analysis methods which can be implemented numerically; furthermore, these methods can yield estimates of the Q of an eccentric feed in terms of how well it synthesizes a desired field distribution. Section 2 contains a detailed discussion of the circular-cylindrical case and Section 3 contains a brief description of the spherical case.

2. Synthesis of Circular-Cylindrical Waves by an Eccentric Feed

The addition theorem for Bessel functions provides an exact method to synthesize a given field distribution on a circular cylinder as a sum of circular-cylindrical waves radiating from an eccentric center located within the cylinder; the theorem also provides an exact method to analyze a field distribution on a circular cylinder which is produced by a given sum of circular-cylindrical waves radiating from an eccentric center located within the cylinder.[3] The theorem determines restrictions on the size of the cylinder, and displacement of the eccentric center, in order that the synthesis method be valid.

A two-dimensional view of the geometry is shown in Fig. VI-4; the axes of the eccentric cylinders, O and O', are parallel to the z axis of a Cartesian coordinate system and are separated by a distance d. The synthesis results are summarized as follows.

1. A field distribution consisting of a finite number of circular-cylindrical waves radiating from O can be synthesized by an infinite sum of circular-cylindrical waves radiating from an eccentric axis O'; this sum converges only outside a cylinder of convergence for synthesis as shown in Fig. VI-4.

2. A field distribution consisting of a finite number of circular-cylindrical waves radiating from O can be synthesized approximately to any degree of precision less than 100% by a finite sum of circular-cylindrical waves radiating from an eccentric axis O'; this sum converges everywhere except at O'.
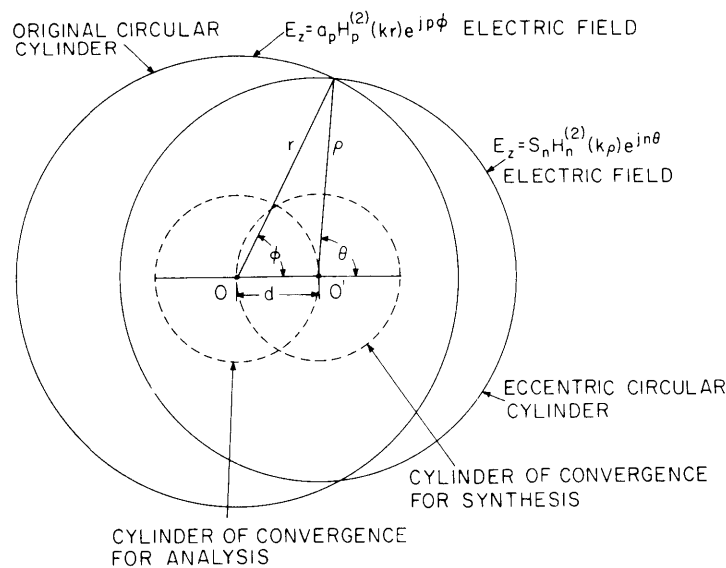

Fig. VI-4. Geometry of concentric and eccentric coordinate systems.

The previous statements are also true when O is taken as the eccentric axis with respect to O'; this case is termed "analysis" since it will be employed to analyze the approximate synthesis method. The previous statements hold separately for waves whose electric field is polarized in the z direction, TE waves, and waves whose magnetic field is polarized in the z direction, TM waves. The exact method is written in terms of the complex wave amplitudes as follows:

Synthesis
$$S_n = \sum_p a_p J_{p-n}(kd)$$
(1)

Analysis
$$a_p = \sum_{n=-\infty}^{-\infty} S_n J_{p-n}(kd)$$
(2)

where S_n is the complex amplitude of the nth wave radiating from O', a_p is the complex amplitude of the pth wave radiating from O, $J_{p-n}(kd)$ is a Bessel function of integral order (p-n) and argument kd, and k is the propagation constant of free space. The electric field of TE waves radiating from O is given by

$$E_z = \sum_p a_p H_p^{(2)}(kr) \, e^{jp\phi}$$
(3)

and the electric field of TE waves radiating from O' is given by

$$E_z = \sum_{n=-\infty}^{\infty} S_n H_n^{(2)}(k\rho) \, e^{jn\theta}$$
(4)

where $H_p^{(2)}(kr)$ denotes a Hankel function of the first kind of integral order p, and (r, ϕ) and (ρ, θ) are circular-cylindrical coordinates shown in Fig. VI-4. The addition theorem shows that the fields expressed by Eqs. 3 and 4 are identical everywhere on and outside a cylinder of convergence for synthesis as shown in Fig. VI-4, if Eq. 1 is satisfied for all n; inside the cylinder of convergence Eq. 4 diverges. Therefore, in order to synthesize a field distribution given by Eq. 3 exactly by waves radiating from an eccentric center, the displacement of the center must be less than r/2

$$d \leqslant (r/2).$$
(5)

An approximate synthesis procedure is obtained by choosing 2N + 1 terms of Eq. 4 whose amplitudes are given by Eq. 1

$$E_z = \sum_{n=-N}^{N} S_n H_n^{(2)}(k\rho) \, e^{jn\theta}.$$
(6)

Equation 6 represents a field distribution which converges everywhere except at O';
therefore, for the approximate method Eq. 5 is replaced by the weaker restriction

$$d \leq r. \tag{7}$$

The degree to which Eq. 6 equals Eq. 3 can be found by applying the analysis relation,
Eq. 2, to $2N+1$ terms of S_n in order to compute the complex amplitude of the synthe-
sized waves a'_p

$$a'_p = \sum_{n=-N}^{N} S_n J_{p-n}(kd) \tag{8}$$

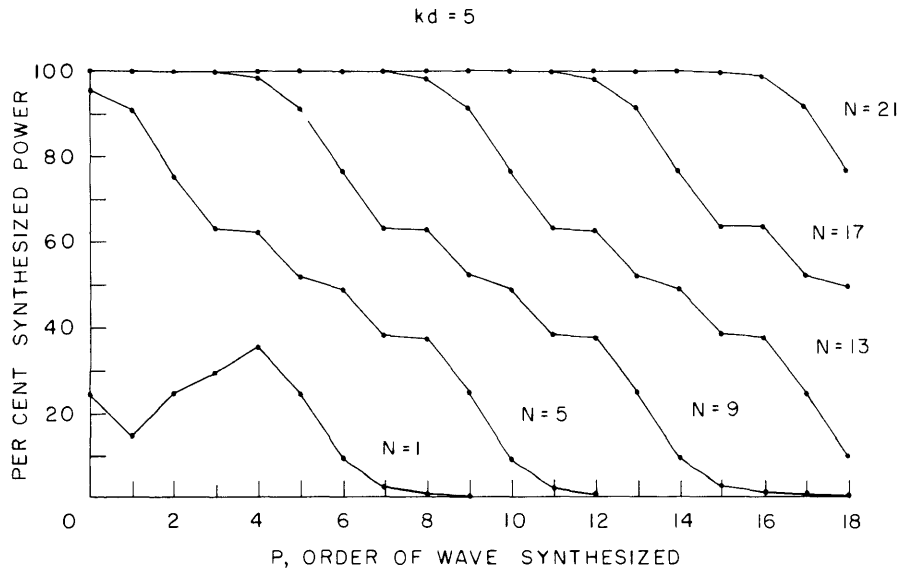and compare the values with the desired a_p; another comparison is the ratio of the power

kd = 5

Fig. VI-5. Per cent of power synthesized for a single wave vs order for
kd = 5 and N = 1, 5, 9, 13, 17, 21.

carried by the synthesized waves P_s to the power carried by the desired waves, P_o, R,
where

$$R = 100(P_s/P_o)\% \tag{9}$$

and

$$P_s = (2/kZ_o) \sum_{n=-N}^{N} |S_n|^2 \quad W/M \tag{10}$$

$$P_o = (2/kZ_o) \sum_p |a_p|^2 \quad W/M. \tag{11}$$

Z_o is equal to the characteristic impedance of free space. For exact synthesis R = 100%. R is plotted in Fig. VI-5 for the case of a single wave of order p radiating from O and kd = 5; in order for R to be at least 98%, N must exceed kd + p. The Q of a feed that synthesizes a finite number of circular-cylindrical waves radiating from O' is high if the circumference per wavelength, (kρ), of the smallest cylinder concentric with O' that encloses the feed is less than the maximum order of the wave radiated, N.[4]

3. Synthesis of Spherical Waves by an Eccentric Feed

The translational addition theorems for spherical vector waves provide an exact method to synthesize a given realizable field distribution on a sphere in terms of a set of spherical waves radiating from an eccentric center located within the sphere.[5,6] The results for the sphere are similar in all respects to those of the circular cylinder which were presented above and will not be repeated. This section will be concerned only with the restatement of Cruzan's results in a form appropriate for the synthesis problem.

The geometry is identical to that shown in Fig. VI-4; the eccentric coordinate system is obtained by translating the original coordinate system parallel to itself a distance d along the z axis. The spherical coordinates in the original system are defined by (r, θ, ϕ) and in the eccentric system by (r', θ', ϕ). The addition theorem for spherical vector waves is based on the addition theorem for spherical scalar waves

$$h_n^{(2)}(kr) \, P_n^m(\cos \theta) \, e^{jm\phi} = \sum_{\nu=0}^{\infty} A(m, \nu) \, h_\nu^{(2)}(kr') \, P_\nu^m(\cos \theta') \, e^{jm\phi}, \tag{12}$$

where $h_n^{(2)}$ is a spherical Hankel function of the first kind, P_n^m is an associated Legendre function. The coefficients $A(m, \nu)$ can be obtained from the following integral which is obtained by equating the far zone fields given by Eq. 12

$$A(m, \nu) = j^{n-\nu} \frac{\int_0^\pi e^{-jkd \cos \theta} \, P_n^m(\cos \theta) \, P_\nu^m(\cos \theta) \sin \theta \, d\theta}{\int_0^\pi \left(P_\nu^m(\cos \theta) \right)^2 \sin \theta \, d\theta} \tag{13}$$

or by means of the following series which involves the Wigner 3-j symbols $\begin{pmatrix} l_1 & l_2 & l_3 \\ m_1 & m_2 & m_3 \end{pmatrix}$

$$A(m, \nu) = \sum_{p=0}^{\infty} j^{n-\nu-p}(2p+1)(2\nu+1) \, j_p(kd)(-1)^m \sqrt{\left(\frac{(n+m)!}{(n-m)!}\right)\left(\frac{(\nu-m)!}{(\nu+m)!}\right)} \begin{pmatrix} p & n & \nu \\ 0 & 0 & 0 \end{pmatrix} \begin{pmatrix} p & n & \nu \\ 0 & m & -m \end{pmatrix} \tag{14}$$

The spherical vector wave functions are given in terms of two vector wave functions $\overline{M}_{mn}$ and $\overline{N}_{mn}$ where

$$\overline{M}_{mn} = \left(\frac{jm}{\sin\theta} P_n^m(\cos\theta) \overline{i}_\theta - \frac{dP_n^m(\cos\theta)}{d\theta} \overline{i}_\phi \right) h_n^{(2)}(kr) \, e^{jm\phi} \tag{15}$$

$$k\overline{N}_{mn} = \nabla \times \overline{M}_{mn}. \tag{16}$$

The addition theorems which can be used to synthesize $\overline{M}_{mn}$ and $\overline{N}_{mn}$ are then given by

$$\overline{M}_{mn}(r, \theta, \phi) = \sum_{\nu=0}^{\infty} \left(A_{m\nu}^{mn} \overline{M}_{m\nu}(r', \theta', \phi) + B_{m\nu}^{mn} \overline{N}_{m\nu}(r', \theta', \phi) \right) \tag{17}$$

$$\overline{N}_{mn}(r, \theta, \phi) = \sum_{\nu=0}^{\infty} \left(A_{m\nu}^{mn} \overline{N}_{m\nu}(r', \theta', \phi) + B_{m\nu}^{mn} \overline{N}_{m\nu}(r', \theta', \phi) \right), \tag{18}$$

where the complex wave coefficients are written in Cruzan's notation and are explicitly given by

$$A_{m\nu}^{mn} = A(m, \nu) + \frac{k}{\nu(\nu+1)} \left(\frac{(\nu+1)(\nu-m)}{2\nu-1} A(m, \nu-1) + \frac{\nu(\nu+m+1)}{2\nu+3} A(m, \nu+1) \right) \tag{19}$$

$$B_{m\nu}^{mn} = \frac{jkm}{\nu(\nu+1)} A(m, \nu). \tag{20}$$

Relations (19) and (20) can be derived by equating the far-zone fields given by Eqs. 17 and 18 and by using the orthogonality relations of the $\overline{M}_{mn}$ and $\overline{N}_{mn}$ angular functions. The addition theorems which are useful for analyzing waves radiating from the eccentric center are obtained by interchanging primed and nonprimed coordinates in Eqs. 17 and 18 and replacing d by -d in Eq. 14.

Use of the addition theorem for spherical vector waves requires the computation of $A(m, \nu)$ by means of Eq. 13 or the series given by Eq. 14. The series is composed of a finite number of nonzero terms because of special properties of the 3-j symbols; these can be evaluated using various recursion relations.[7]

J. I. Glaser

References

1. J. I. Glaser, "Use of the Lorentz Reciprocity Theorem for the Design and Evaluation of Feeds for Reflectors," presented at the 1969 USNC-URSI Spring Meeting, Washington, D.C., April 22, 1969.

2. L. J. Ricardi, "A Method of Synthesizing the Fields of a Feed for a Spherical Reflector," Sc. D. Thesis, Department of Electrical Engineering, Northeastern University, Boston, Mass., May 1969.

3. G. N. Watson, A Treatise on the Theory of Bessel Functions (Cambridge University Press, London), 1966, p. 361.

4. L. J. Chu, "Physical Limitations of Omni-directional Antennas," J. Appl. Phys. 19, 1163-1175 (1948).

5. S. Stein, "Addition Theorems for Spherical Wave Functions," Quart. Appl. Math. 19, 15-24 (1961).

6. O. Cruzan, "Translational Addition Theorems for Spherical Vector Wave Functions," Quart. Appl. Math. 20, 33-40 (1962).

7. A. R. Edmonds, Angular Momentum in Quantum Mechanics (Princeton University Press, Princeton, N.J.), 1957.

D. QUANTIZATION OF ELECTROMAGNETIC RADIATION FIELDS IN MOVING UNIAXIAL MEDIA

Radiation fields in moving uniaxial media have been quantized without introducing auxiliary potential functions. Hamiltonian and momentum operators are diagonalized in momentum space and written in terms of annihilation and creation operators of the photon state. It has been found that two types of photons corresponding to classical ordinary and extraordinary waves will exist, and they are called "ordinary photons" and "extraordinary photons." Physical interpretations of the various results are discussed in a paper that has been submitted to the Journal of Applied Physics.

J. A. Kong